Mühendislik Bilimleri ve Tasarım Dergisi
12(4), 663-675, 2024
e-ISSN: 1308-6693

Journal of Engineering Sciences and Design
DOI: 10.21923/jesd.1541595

Araştırma Makalesi Research Article

EFFECTS OF ASYMMETRICAL STATOR STRUCTURE ON BLDC MOTOR PERFORMANCE FOR HOUSEHOLD APPLIANCES

Emin Tarik KARTAL, Fatma KESKIN ARABUL*

Yildiz Technical University, Department of Electrical Engineering, Istanbul, Türkiye

Keywords

Electrical Machines, Brushless DC Motor, Cogging Torque, Torque Ripple, Finite Element Analysis.

Abstract

Brushless direct current motors (BLDCM) have been frequently preferred in the industry, especially in home appliances, due to their advantages such as long life, high efficiency, low maintenance costs and ease of control. In addition to these advantages, the main disadvantages of these motors are known to be high torque ripple and vibration levels. In this study, alternative asymmetric designs are realized in the stator tooth structure of the BLDCM designed for home appliances, and comparative analyses of the effects of the non-uniform air gap caused by the asymmetric tooth structure on the motor performance are presented. Two different asymmetric structures, namely the model with clockwise asymmetric design (CW) and the model with counterclockwise asymmetric design (CCW) in the stator tooth structure, are determined in the stator design. With these alternative designs, improvements are made in terms of torque ripple and cogging torque when compared with the reference motor; notably, the CCW-2 model achieves the lowest ripple at 19.4% compared to 23.1% for the reference motor, and a 42% reduction in cogging torque. The design of the motor models is made in ANSYS EDT program as two dimensional (2D) and analyzed with the Finite Element Method (FEM). In the analysis results, air gap flux density, torque, torque ripple and cogging torque are examined, and the flux density and torque spectrum obtained by Fast Fourier Transform (FFT) are presented comparatively.

EV ALETLERİ İÇİN ASİMETRİK STATOR YAPISININ BLDC MOTOR PERFORMANSINA ETKİLERİ

Anahtar Kelimeler

Elektrik Makinaları, Fırçasız DC Motor, Vuruntu Momenti, Moment Dalgalanması, Sonlu Elemanlar Analizi.

Öz

Fırçasız doğru akım motorları uzun ömür, yüksek verim, düşük bakım maliyetleri ve kontrol kolaylığı gibi avantajları nedeniyle endüstride özellikle ev aletlerinde sıklıkla tercih edilmektedirler. Bu avantajlarının yanı sıra, moment dalgalanması ve titreşim seviyelerinin yüksek olması bu motorların başlıca dezavantajları olarak bilinmektedir. Bu çalışmada, ev aletleri için tasarlanan fırçasız doğru akım motorun stator diş yapısında alternatif asimetrik tasarımlar gerçekleştirilmiş ve asimetrik diş yapısının neden olduğu düzgün olmayan hava aralığının motor performansı üzerindeki etkilerinin karşılaştırmalı analizleri sunulmuştur. Stator diş yapısında saat yönünde asimetrik tasarıma sahip model (CW) ve saat yönünün tersine asimetrik tasarıma sahip model (CCW) olmak üzere iki farklı asimetrik yapı stator tasarımında belirlenmiştir. Bu alternatif tasarımlarla, referans motorla karşılaştırıldığında moment dalgalanması ve vuruntu momenti açısından iyileştirmeler yapılmaktadır; özellikle CCW-2 modeli, referans motor için %23,1'e kıyasla %19,4 ile en düşük dalgalanmayı ve vuruntu momentinde %42'lik bir azalma elde etmektedir. Motor modellerinin tasarımı ANSYS EDT programında iki boyutlu olarak yapılmış ve Sonlu Elemanlar Yöntemi ile analiz edilmiştir. Analiz sonuçlarında hava aralığı akı yoğunluğu, moment, moment dalgalanması ve vuruntu momenti incelenmiş, Hızlı Fourier Dönüşümü ile elde edilen akı yoğunluğu ve moment spektrumu karşılaştırmalı olarak sunulmuştur.

Alıntı / Cite

Kartal, E, T., Keskin Arabul, F., (2024). Effects of Asymmetrical Stator Structure on BLDC Motor Performance for Household Appliances, Journal of Engineering Sciences and Design, 12(4), 663-675.

Yazar Kimliği / Author ID (ORCID Number)
E. T. Kartal, 0000-0002-4966-7258
F. Keskin Arabul, 0000-0002-9573-8440

Makale Süreci / Article Process	
Başvuru Tarihi / Submission Date	31.08.2024
Revizyon Tarihi / Revision Date	11.10.2024
Kabul Tarihi / Accepted Date	16.10.2024
Yayım Tarihi / Published Date	25.12.2024

* İlgili yazar / Corresponding author: fkeskin@yildiz.edu.tr, +90-212-383-5848

EFFECTS OF ASYMMETRICAL STATOR STRUCTURE ON BLDC MOTOR PERFORMANCE FOR HOUSEHOLD APPLIANCES

Emin Tarik KARTAL, Fatma KESKIN ARABUL†
Yildiz Technical University, Department of Electrical Engineering, Istanbul, Türkiye

Highlights

- FEM and FFT are employed to evaluate the performance of BLDCMs with asymmetric stator designs, focusing on torque ripple and cogging torque.
- CW designs enhanced output torque but increased torque ripple and vibrations, potentially impacting motor stability.
- CCW designs successfully reduced torque ripple, cogging torque, and vibrations, resulting in improved overall motor efficiency and performance.

Purpose and Scope

This paper aims to address the high torque ripple and vibration levels in BLDCMs, which are commonly used in home appliances. The research focuses on improving motor performance by designing asymmetric stator tooth structures and analyzing their effects on torque ripple and cogging torque. The study evaluates two asymmetric designs, CW and CCW models, using FEM.

Design/methodology/approach

The study employs FEM using the ANSYS EDT program to design and evaluate BLDCMs with asymmetric stator tooth structures. Two asymmetric designs, CW and CCW, are analyzed to compare their effects on air gap flux density, torque, and torque ripple. The approach includes modeling the motors in 2D and examining the impact of non-uniform air gaps on performance metrics. The theoretical scope involves analyzing electromagnetic characteristics and optimizing motor design for reduced torque ripple. To better understand performance, FFT is applied to analyze the frequency domain characteristics of the air gap flux density and torque ripple, providing insights into harmonic components and their influence on overall motor performance.

Findings

The CW-2 model results in the highest torque ripple at 33.1%, compared to the reference motor's 23.1%, while showing a 25.5% reduction in the fundamental air gap flux density component. The CCW-2 model achieves the lowest torque ripple at 19.4% and a 42% reduction in cogging torque compared to the reference motor. These findings indicate that asymmetric stator designs can enhance motor performance, with the CW models increasing torque but also ripple, and the CCW models offering better overall performance by reducing both ripple and cogging torque.

Practical implications

The study's findings suggest that asymmetric stator designs can improve BLDCM performance in household appliances by reducing torque ripple and cogging torque. Implementing these designs could lead to quieter and more efficient motors with lower maintenance costs. The improvements could contribute to cost savings and better user experience in appliance operation.

Originality

The paper introduces novel asymmetric stator tooth structures for BLDCMs, distinguishing it from existing research. It provides a comparative analysis of CW and CCW models, offering insights into how these designs affect torque ripple and cogging torque. The findings contribute to the development of more efficient and quieter BLDCMs, presenting a valuable alternative to conventional designs.

† Corresponding author: fkeskin@yildiz.edu.tr, +90-212-383-5848

1. Introduction

In recent years, BLDCMs have become highly preferred in the industry (Wang et al., 2021). BLDCM confer several advantages over other types of electric motors, such as brushed motors. They facilitate enhanced speed control, provide high efficiency, possess a longer operational lifespan, exhibit a high torque-to-weight and torque-to-watt ratio, enhanced reliability . BLDCM differ from brushed direct current motors in that they utilize electronic commutation, eliminating the need for mechanical commutation and friction, which leads to higher efficiency, reduced maintenance, and less electromagnetic interference. Common applications where BLDC motors are widely preferred include household appliances, electric bicycles, robots and actuators, the aerospace-defense industry, and fans and pumps (Prakash & Naveen, 2023). In particular, BLDCMs are known to be alternatives to brushed direct current motors, universal motors, and single-phase induction motors, especially in electric household appliances such as tumble dryers and washing machines, as well as in fans and blowers (Mohanraj, Aruldavid, et al., 2022). The most influential factors in this preference include the efficiency, noise, and vibration level limits required by the standards in the white goods industry (Mohanraj, Aruldavid, et al., 2022). However, today's popular research topics such as energy efficiency, sustainable environment and production, and eco-friendly technologies continue to be important for electric household appliances as well.

When considering comfort, noise, vibration and performance, torque ripple has an important effect on the BLDCM. Torque ripple in BLDCMs leads to increased acoustic noise, undesirable speed ripple, and prevents the motor from achieving high performance. It can also cause poor quality of speed-torque characteristics, noise, vibrations, and faults in motor drives (Prabhu et al., 2023), (Mohanraj, Aruldavid, et al., 2022).

The key factors influencing torque ripple in BLDCMs encompass a wide range of design and control aspects, including modulation strategies, motor design considerations, eccentricities, control techniques, and voltage/current control strategies (Mohanraj, Gopalakrishnan, et al., 2022), (Liu et al., 2005), (Shi et al., 2017). The stator slot shape, stator slot opening width, winding pattern, commutation strategy, rotor design, stator and rotor skewing all play crucial roles in influencing torque ripple in BLDCMs (Prabhu et al., 2023), (Huang et al., 2012), (Rahman et al., 2014).

A given study proposes a method to reduce torque ripple in interior permanent magnet BLDCMs using a modified rotor design. The analysis, based on 2D using FEM simulations, shows that this approach is more advantageous from a manufacturing perspective compared to rotor step skewing. Results reveal a reduction in torque ripple and an increase in average torque (Raja & Geethalakshmi, 2018).

A recent study highlights the advantages of BLDCMs for battery electric vehicles, focusing on reducing torque ripples caused by high cogging torque, which can create noise and vibrations. The research employs a parametric technique to optimize the rotor pole embrace factor and magnetic thickness, significantly decreasing cogging torque. Using the ANSYS Maxwell tool, the design achieves a 5.7% increase in efficiency compared to the base model, along with fewer torque ripples (Rupam et al., 2022).

The paper discusses the design of stator and rotor shapes in interior permanent magnet BLDCMs to reduce torque fluctuations. A modified rotor with unequal outer diameter and pole shoe adjustments creates a partly enlarged air gap, leading to reduced torque ripple by enhancing torque values at minimum positions. The final designs are determined through a design of experiments process, while magnetic field and torque characteristics are analyzed using 2D FEM and validated by experimental results (Lee et al., 2012).

In a study where design optimization is emphasized, structural optimization based on the level set method is formulated to reduce torque ripples in an interior permanent magnet motor, which experiences significant torque ripple due to reluctance torque, leading to noise and vibration. The method minimizes the difference between torque values at specific rotor positions and a target average torque while adhering to material constraints. The nonlinear ferromagnetic material boundary of the stator is represented through an embedded level set function, with boundary movement driven by optimality and convergence conditions. This approach is applied to design optimal stator configurations for a hybrid electric vehicle's traction motor, resulting in improved torque characteristics (Kwack et al., 2010).

A given paper explores the impact of magnet shape on torque behavior in surface-mounted permanent magnet (SPM) motors. Analyzing pole embrace optimization, magnet skew, and magnet shaping across various 8-pole, 24-slot, three-phase SPM motors, the study uses the FEM to predict back-EMF and torque ripple. Results indicate that magnet skew effectively reduces cogging torque, while shaping with the third harmonic increases average torque and achieves lower torque ripple compared to sine magnet shaping and optimized pole embrace (Lin et al., 2014).

A recent paper examines the use of slitted stator core teeth geometry to reduce torque ripples in permanent magnet synchronous motors (PMSMs), which are widely used in traction applications. Despite their energy-saving benefits, PMSMs typically face torque ripple issues, which can be mitigated through magnetic core design and current control methods. An outer rotor PMSM is utilized for performance comparisons, with two numerical models developed: a classical analytical model and a slitted stator core model. Using FEM, the study reveals that the slitted core PMSM exhibits a 6% reduction in torque ripple and an increase of 3 Nm in average torque compared to the traditional outer rotor PMSM (Tezcan & Yetgin, 2023).

Finite control set model predictive control (FCS-MPC) is utilized to reduce torque ripple in BLDCMs. The approach optimizes duty cycles and switching states, enhancing performance, especially at high speeds. Validation through experimental results confirms its effectiveness, addressing challenges such as parameter mismatches and high-speed PWM regulation (Li et al., 2024).

Auxiliary step-up circuits are proposed to reduce torque ripple in BLDCMs during commutation, a key issue in high-performance applications. The circuit charges a capacitor during non-commutation and boosts DC-bus voltage during commutation. This method enhances energy efficiency, reduces power component capacity, and shortens commutation time (Yao et al., 2019).

Commutation torque ripple in BLDCMs operating in six-step driving mode is addressed through a study that analyzes torque ripple causes and proposes a suppression model using phase current prediction based on trapezoidal back EMF. A pulse width modulation (PWM) model predictive control algorithm is introduced to adjust the duty cycle, reducing torque ripple without altering the motor's driving circuit topology (Xia et al., 2020).

Switching loss and torque ripple in BLDCMs are reduced by combining two- and three-phase switching strategies. The conventional two-phase switching reduces loss in the conduction region, while a modified three-phase switching strategy with voltage compensation minimizes torque ripple during commutation. The method optimizes the phase current slope using back EMF and phase voltage, assuming a sinusoidal back EMF slope (Park & Lee, 2020).

Maximum Torque per Ampere (MTPA) control is proposed for surface-mounted BLDCMs to address iron loss effects. Ignoring iron loss causes torque errors and fails to track minimum current. The proposed system compensates for iron loss, minimizing torque ripple and ensuring effective MTPA realization (Khazaee et al., 2021).

Improved switching table-based direct torque control techniques are introduced with a nine-level hysteresis band to reduce torque ripple in permanent magnet BLDCMs. By using three lookup tables for varying torque errors, the method reduces computational cost, improves dynamic response, and minimizes high-frequency components (Karan et al., 2024).

Predictive current control strategies for permanent magnet BLDCMs are evaluated, focusing on deadbeat, hysteresis-based, and FCS-MPC methods in the stationary plane. A 48V, 660W motor is tested, and results show that predictive control outperforms PI-PWM by reducing commutation torque ripple, controlling current harmonics, and enhancing torque-speed characteristics, particularly in the constant torque zone (Trivedi & Keshri, 2020).

The design parameters influencing torque ripple in BLDCMs include pole embrace factor, magnet thickness, and various stator and rotor design parameters. Electromagnetic design optimization, including FEM, and control techniques play a crucial role in minimizing torque ripple and improving system performance and efficiency. Current research trends involve exploring advanced controller designs and analyzing the impact of different PWM modes on torque ripple. In this study, which is an alternative to the recent literature in terms of electromagnetic design, an outer rotor BLDCM is designed for electrical household appliances such as fan-blowers and tumble dryers. Ferrite permanent magnet material is preferred in order not to exceed cost limits. Subsequently, in the designed BLDCM, improvements are made in terms of output torque and torque ripple. In alternative designs, the outer rotor BLDCM has an asymmetric structure on the stator, while the effect of non-uniform air gap on torque and torque ripple is examined in the study. In the designs, not only the torque but also the the effects of the non-uniform air gap on the cogging torque are also evaluated. As a result, the stator geometry that minimizes torque ripple is determined. While the improved motor structure has a cost advantage, it becomes apparent as a good alternative to the reference motor in terms of undesirable noise and vibration components. The remainder of the paper is organized as follows: Section 2 describes Material and Method. Section 3 introduces Proposed Method. In Section 4, the analysis results are presented and evaluated comparatively. Finally, Section 5 finalizes the study with the concluding remarks.

2. Material and Method

In this section, the 2D model of the reference convensional BLDC motor designed for electrical household appliances and fan applications is analysed with FEM in ANSYS program. In general, the design of an electric machine involves five key theoretical areas: electrical, magnetic, dielectric, thermal, and mechanical. Electrical; voltage, frequency, and phase specifications are crucial for compatibility with the power supply, alongside determining connection types (star or delta), winding configurations, and factors such as current density, copper losses, and short-circuit current. Magnetic; this includes setting maximum flux densities, calculating iron losses, addressing saturation effects, magnetizing and leakage inductances, and determining slot and tooth shapes to manage harmonic effects. Dielectric; the design must consider insulation thickness to withstand continuous and surge voltages, as well as proper routing of windings and bushing selection to prevent flashovers. Thermal; effective heat management is essential to prevent machine failure, requiring appropriate coolant selection, duct design, fan design, and temperature rise calculation. Mechanical considerations include calculating critical rotational speeds, acoustic vibrations, mechanical stresses, moment of inertia, and forces on windings, especially during short circuits (Lipo, 2017).

The dimensions of electrical machines are often described by "torque per rotor volume" (TRV), which relies on the product of electrical loading (A) and magnetic loading (B). The concept that "torque is the product of current and flux" highlights why the AB combination is crucial. Both A and B are restricted by material properties, and even with the best materials, they are further constrained by heat generation and cooling capacity (Hendershot & Miller, 2010) (Lipo, 2017).

The electrical loading A is defined as in Equation (1) the current density around the air gap circumference, that is, number of ampere conductor per metre around the stator surface that faces the air gap.

$$\mathrm{A} = \frac{\text{Total ampere conductors}}{\text{Air gap circumference}} = \frac{2mT_{ph}I}{\pi D} \ \ A/m \qquad (1)$$

Where, I is the RMS phase current, m is the number of phases, T_{ph} is the number of turns in per phase, D is the diameter of the air gap. The air gap is assumed to be small compared to the rotor diameter, so that no distinction is made between the rotor diameter and the stator diameter. The RMS current is used because it determines the I^2R heating, which is what limits the electrical loading (Hendershot & Miller, 2010).
The magnetic loading B is defined as the maximum value fundamental component of flux density in the air gap. In motors the fundamental flux per pole (Φ_1) is given in Equation (2).

$$\Phi_1 = B\ x\ \frac{\pi DL}{2p} x\ \frac{2}{\pi}\ Wb \qquad (2)$$

Where, p is the number of the pole pairs and L is the axial length. The induced RMS electromotive force (E) per phase is given in Equation (3) by the standart equation.

$$\mathrm{E} = \frac{2\pi k_{w1} T_{ph} \Phi_1 f}{\sqrt{2}} = \frac{\pi^2 k_w T_{ph} BLf}{\sqrt{2}\, p}\ V \qquad (3)$$

Where, f is the fundamental frequency, k_{w1} is the fundamental winding factor. The maximum available electromagnetic power at the air gap is mEI, and if all this is converted into mechanical power $T\omega_M$, It is possible to obtain Equation (4).

$$\mathrm{TRV} = \frac{T}{V_r} = \frac{2AB}{\sqrt{2}}\ \ N/m^2 \qquad (4)$$

According to this, ω_M is the mechanical angular speed in rad/sec and V_r is the rotor volume that $\pi^2 DL/4$ are known. There it is necessary to define the magnetic shear stress (σ), which is given in Equation (5).

$$\mathrm{TRV} = \frac{T}{V_r} = 2\sigma\ \ N/m^2 \qquad (5)$$

The TRV is connected to the magnetic shear stress σ, which represents the tangential force per unit area of the rotor's swept surface.

In Equation (5) it represents the product of the surface current density and the air gap flux density and is often used as a value figure for comparing machines. The magnetic shear stress has nominal units (ampere/metre) × (tesla). However, it appears that in basic units tesla = newton/ (ampere × metre) and thus the product has the basic units newton/metre^2, alternatively called Pascal (Pa). Hence, this quantity is equivalent to a pressure and is appropriately called the magnetic shear stress (Lipo, 2017).

In the consideration of all these design guidelines, the materials, properties and parameters determined for the design of the reference conventional outer rotor BLDCM with ferrite magnetic material are as given in Table 1.

Table 1. Reference motor specifications

Stator outer diameter	84 mm
Rotor inner diameter	85 mm
Rotor outer diameter	100 mm
Axial length	30 mm
Air gap length	0.5 mm
Number of stator slots	9
Number of rotor poles	8
Rated Power	109 W
Rated voltage/phase/connection	48 V/3/Y
Speed (rpm)	750 rpm
Rated phase current	3.6 A
Magnet material	Ferrit/Hitachi-12F-80°C
Electrical steelF	JFE-50JN270

Where, together with the design parameters of the conventional outer rotor BLDCM given as reference in Table 1, the slot pitch in the winding type formed in the stator is one slot and two layer windings are used. There are a total of 130 turns of conductors in the stator slots. In the conductors in all winding structures, 2 stranded round wires with a diameter of 0.607 mm and a maximum insulation diameter of 0.07 mm are used. In addition, there is only one branch in each phase in the stator. Including the slot insulation material, the insulation material between the winding layers and the insulation materials in the slot opening area, the net slot fill is kept at 55%. The 2D model and mesh structure of the designed conventional outer rotor BLDC motor in ANSYS program with the defined specifications are given in Figure 1.

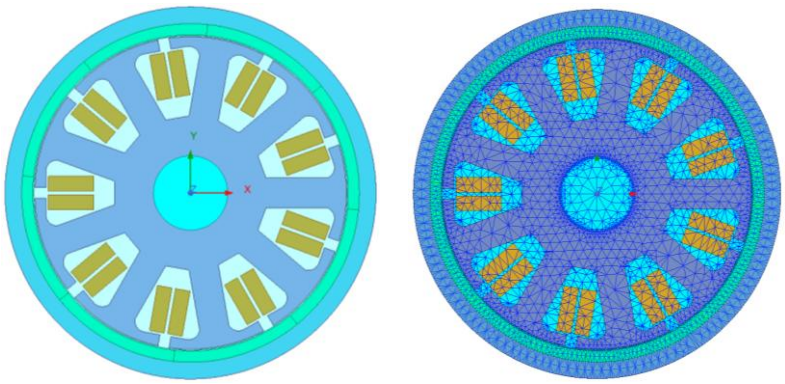

(a) (b)

Figure 1. 2D model of the conventional outer rotor BLDC motor (a) and mesh structure (b)

In the reference conventional motor model given in Figure 1, the net slot area is 214 mm^2 and the material used in the stator windings is copper. Figure 2 shows the magnetic flux density distribution and magnetic field strength distribution obtained from the analyses.

As shown in Figure 2, according to the results of the analysis, the maximum magnetic flux density seen in the conventional BLDC motor stator teeth is 1.5 T and this value is observed in the linear region of the selected electrical steel material. In the stator tooth bottom region, as expected, it forces the value of 1.7 T in specific tight areas. Another important material where magnetic flux density is effective is permanent magnet materials. In this motor with outer rotor structure, the general flux density distribution on the magnet materials on the rotor is around 0.3-0.4 T. It is at 0.2 T values in partially tight areas forced by the magnetic field strength. For these areas; when the demagnetisation curve of the preferred magnetic material is examined, the field strength obtained for

80°C is around 150 kA/m, far from the knee point.

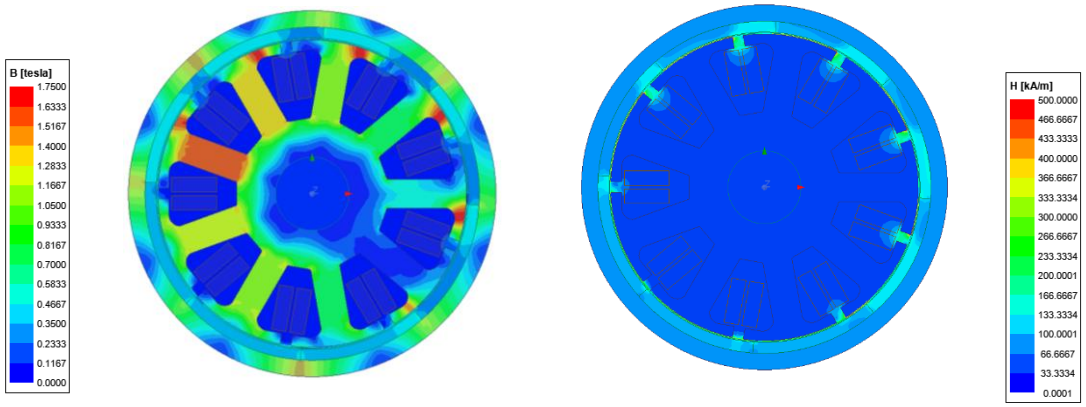

(a) (b)

Figure 2. Results of the flux density (a) and field strength distributions (b) obtained from the analysis of the conventional outer rotor BLDCM

After the evaluation of the field strength and flux density distributions obtained from the analysis results, the performance data of the motor are given. The designed reference conventional outer rotor BLDCM has 1.38 Nm shaft torque and 23.1% torque ripple for 109 W output power. The effective phase current is 3.58 A at rated motor speed. In addition, it should be noted that the conventional six step control method is applied on the control side. This method involves switching the motor phases in a sequence of six steps to control the motor's rotation. The conventional six-step control operates in a 120° conduction mode, where each phase conducts for 120° of the electrical cycle. This results in a quasi-square wave current that aligns with the trapezoidal back EMF, leading to torque ripple during commutation. One of the main limitations of the six-step control is the presence of torque ripple, which can affect the motor's performance and efficiency. This is due to the abrupt changes in current during phase commutation. The maximum current value reached by the reference conventional motor designed in this study within half cycle is 5.5 A, while the minimum current value reached during phase commutation is 3.7 A.

3. Proposed Method

In this section, after the reference conventional outer rotor BLDC motor designed and analysed, alternative model designs with asymmetrical stator tooth structure and non-uniform air gap on the stator side are defined and 2D models are created in order to improve the electromagnetic toorque and torque ripple. The models with asymmetric stator tooth structure and non-uniform air gap are given in Figure 3. All models rotate counterclockwise in the same direction as the reference motor. The rotor rotation direction of the reference motor is taken into consideration while creating models with asymmetric tooth structure. The first of the models with asymmetric tooth structure is the model with clockwise asymmetric design in the stator tooth structure (CW) given in Figure 3 (a) and the model with counterclockwise asymmetric design in the stator tooth structure (CCW) given in Figure 3(b).

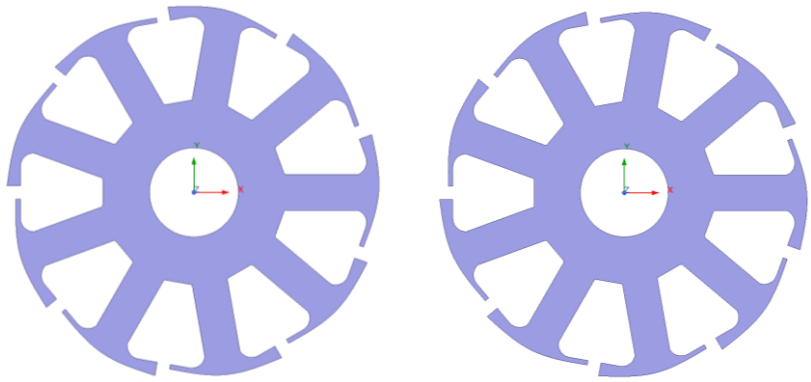

(a) (b)

Figure 3. 2D stator models with asymmetric stator tooth structure (a) CW and (b) CCW

In the reference conventional outer rotor BLDCM, the length determined in the design at the stator tooth bottom ends is 3 mm. However, in the CW and CCW asymmetric stator tooth structures, the stator tooth bottom ends are shortened by 0.4, 0.8, 0.12, 0.16 and 2 mm, and 2D models are created by providing non-uniform air gap with

asymmetric design. Where, the amount of material used in the designs; the amount of electrical steel material used in the rotor, the amount of magnet material and the amount of stator winding copper are equal in all models created. However, the amount of electrical steel used in the stator varies depending on the stator tooth asymmetry.

4. Analysis Results

In this section, together with the reference conventional design BLDC motor, the results of the analysis of air gap flux density, air gap flux density spectrum obtained by FFT analysis, torque, torque spectrum obtained by FFT analysis, torque ripple and cogging torque of the models with asymmetric stator tooth structure and non-uniform air gap are given.

4.1. Analysis Results of CW

The 2D models with asymmetrical stator tooth structure are analysed by FEM and the results are given. The results of the analyses are presented comparatively with the reference design BLDC motor with symmetrical stator tooth structure as CW-0.4 with 0.4 mm shortening at the stator tooth bottom, CW-0.8 with 0.8 mm shortening, CW-1.2 with 1.2 mm shortening, CW-1.6 with 1.6 mm shortening and CW-2 with 2 mm shortening. Figure 4 shows the air gap flux density distribution of the CW models and the reference conventional outer rotor BLDC motor.

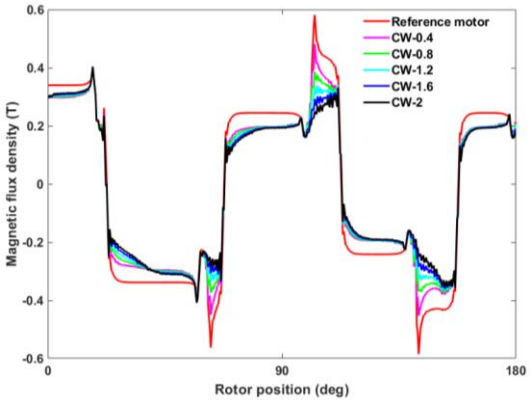

Figure 4. Air gap flux density distribution of CWs

Figure 5 shows the air gap flux density spectrum of the air gap flux density distribution given in Figure 4.

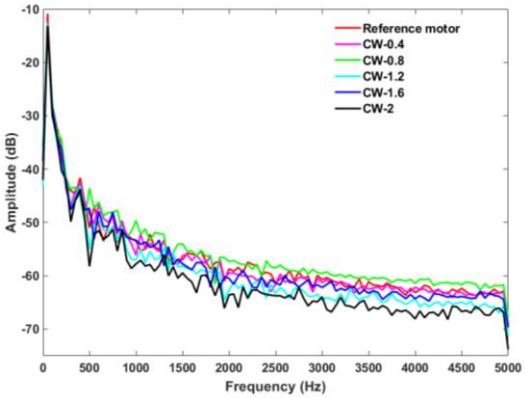

Figure 5. Air gap flux density spectrum of CWs

As shown in Figure 5, when the result of FFT analysis of the air gap flux density is analysed, significant changes are observed in both fundamental and some harmonic components compared to the reference conventional design. In the fundamental component, 14.3% decrease is observed in CW-0.4 model, 18.1% decrease in CW-0.8 model, 19.9% decrease in CW-1.2 model, 23.2% decrease in CW-1.6 model and 25.5% decrease in CW-2 model. In the 300 Hz component of the flux density spectrum, a 30.1% decrease in the CW-0.4 model, a 3.1% increase in the CW-0.8 model, a 33% decrease in the CW-1.2 and CW-1.6 models and a 49% decrease in the CW-2 model are observed compared to the reference motor. Considering these results, the highest decrease in the 300 Hz component is obtained in the CW-2 model. The other important component is 500 Hz. Considering this harmonic component, an increase of 35.7% is observed in CW-0.4 model, an increase of 135.7% in CW-0.8 model, a decrease of 35.7% in CW-1.2 model, an increase of 53.5% in CW-1.6 model and a decrease of 57.1% in CW-2 model compared to the

reference motor. Figure 6 shows the output torque of the CW models and the reference conventional outer rotor BLDCM.

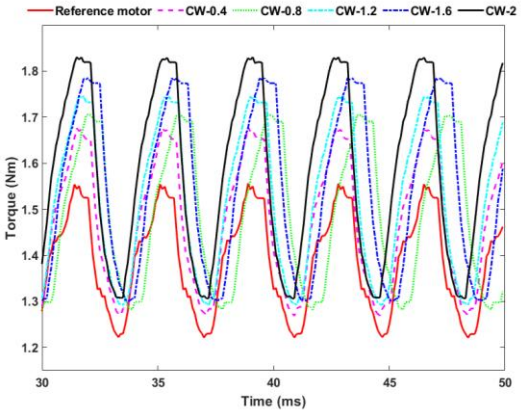

Figure 6. Electromagnetic torque of CWs

As shown in Figure 6, it is concluded that the output torque increases and the torque ripple increases with the shortening length of the asymmetric stator tooth bottom end in the CW structure. The torque and torque ripple in the CW models are given in Table 2.

Table 2. Torque and torque ripples of CWs

	Referance motor	**CW-0.4**	**CW-0.8**	**CW-1.2**	**CW-1.6**	**CW-2**
Torque (Nm)	1.38	1.46	1.49	1.51	1.54	1.57
Torque ripple (%)	23.1	28	28.8	29.8	31.1	33.1

According to the results given in Table 2, the highest output torque with 1.57 Nm is obtained in the CW-2 asymmetric stator tooth structure and an increase of 13.7% is achieved compared to the reference motor. While there is an improvement in the output torque compared to the reference conventional BLDCM, the torque ripple is significantly higher than the reference motor with 33.1% and the torque ripple increases with the increase in asymmetry. Figure 7 shows the torque spectrum of the output torque of the CWs given in Figure 6.

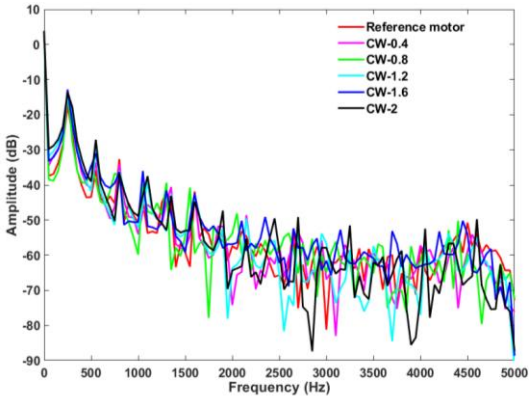

Figure 7. Torque spectrum of CWs

As presented in Figure 7, when the result of the FFT analysis of the electromagnetic torque is analysed, significant changes are obtained in the 250 Hz component of the torque spectrum compared to the reference conventional design. While this harmonic component is 0.136 Nm in the reference motor, it increased by 22.8% at CW-0.4, 52.2% at CW-0.8, 35.2% at CW-1.2, 67.6% at CW-1.6 and 53.6% at CW-2 compared to the reference motor. Another important component for torque ripple is known to be cogging torque. Figure 8 shows the cogging torque of the CW models and the reference conventional outer rotor BLDC motor.

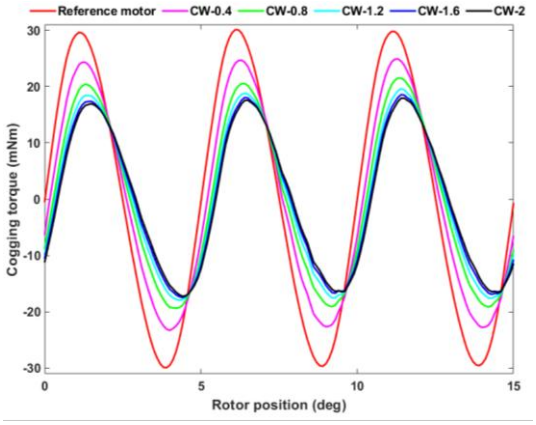

Figure 8. Cogging torque of CWs

According to the cogging torque given in Figure 8, the reference motor has the highest value with 30 mNm. Compared to the reference motor, the cogging torque decreased by 17% in CW-0.4 structure, 28.3% in CW-0.8 structure, 34.6% in CW-1.2 structure, 38.3% in CW-1.6 structure and 40.3% in CW-2 and decreased to 17.9 mNm. Considering all these, it is seen that with the asymmetric tooth structure in the stator, while there is a decrease in cogging torque and an increase in electromagnetic torque in CW models, there is no improvement in torque ripple.

4.2. Analysis Results of CCW

The 2D models with asymmetric stator tooth structure are analysed by FEM and the results are given. The results of the analyses are presented comparatively with the reference design BLDC motor with symmetrical stator tooth structure as CCW-0.4 with 0.4 mm shortening, CCW-0.8 with 0.8 mm shortening, CCW-1.2 with 1.2 mm shortening, CCW-1.6 with 1.6 mm shortening and CCW-2 with 2 mm shortening at the stator tooth bottom. Figure 9 shows the air gap flux density distribution of the CCW models and the reference conventional outer rotor BLDC motor.

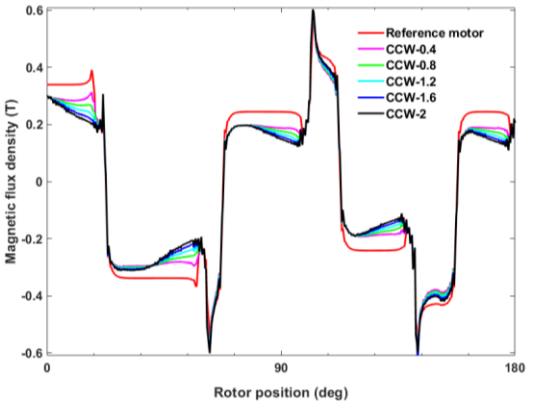

Figure 9. Air gap flux density distribution of CCWs

Figure 10 shows the air gap flux density spectrum of the air gap flux density distribution given in Figure 9.

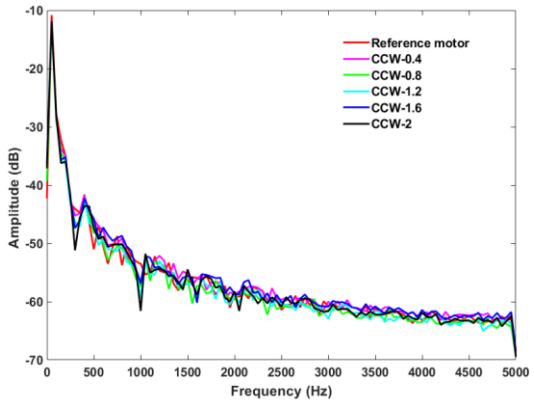

Figure 10. Air gap flux density spectrum of CCWs

As it is given in Figure 10, when the result of FFT analysis of the air gap flux density is analysed, significant changes are observed in both fundamental and some harmonic components compared to the reference conventional design. Compared to the reference motor, the fundamental component decreases by 10.9% in CCW-0.4 model, 12.4% in CCW-0.8 model, 11.9% in CCW-1.2 model, 11.2% in CCW-1.6 model and 12.3% in CCW-2 model. In the CW models, the fundamental component shows a decrease of approximately 25%, while this value is kept at 12% in the CCW structure. In the 300 Hz component of the flux density spectrum, a 12.7% decrease is seen in the CCW-0.4 model, a 33.3% decrease in the CCW-0.8 model, a 23.8% decrease in the CCW-1.2 model, a 31.7% decrease in the CCW-1.6 model and a 55.5% decrease in the CCW-2 model compared to the reference motor. Considering these results; similar to the CW models, the maximum reduction in the 300 Hz component is observed in the CCW-2 model. While the 500 Hz component shows itself in CW models, 1000 Hz appears in CCW models. Considering this harmonic component, a 28.5% reduction is observed in the CCW-0.4 model, approximately 33% in the CCW-0.8 and CCW-1.6 models, 47.6% in the CW-1.2 model and 60.5% in the CCW-2 model compared to the reference motor. Figure 11 shows the output torque of the CCW models and the reference conventional outer rotor BLDC motor.

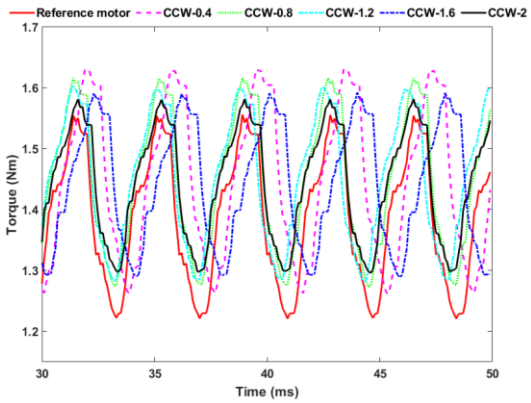

Figure 11. Electromagnetic torque of CCWs

As seen in Figure 11, it is observed that the increase in the shortening length at the end of the asymmetric stator tooth bottom in the CCW structure provides an increase of approximately 4% in the output torque in all CCW models; at the same time, it is seen that the torque ripple is also reduced. Accordingly, the torque and torque ripple in CCW models are given in Table 3.

Table 3. Torque and torque ripples of CCWs

	Referance motor	CCW-0.4	CCW-0.8	CCW-1.2	CCW-1.6	CCW-2
Torque (Nm)	1.38	1.44	1.44	1.44	1.43	1.43
Torque ripple (%)	23.1	25	23.6	22.2	20.8	19.4

As presented in Table 3, there is no significant torque increase in all models in CCW structure compared to the motor with symmetrical stator tooth structure. With the asymmetric stator tooth structure, improvement in torque ripple is achieved in the CCW structure. While the torque ripple in CCW-0.4 and CCW-0.8 models are higher than the reference motor, the torque ripple in CCW-1.2, CCW-1.6 and CCW-2 models decreased below the reference conventional design and reduced to 19.4%. Figure 12 shows the torque spectrum of the output torque of the CCWs given in Figure 11.

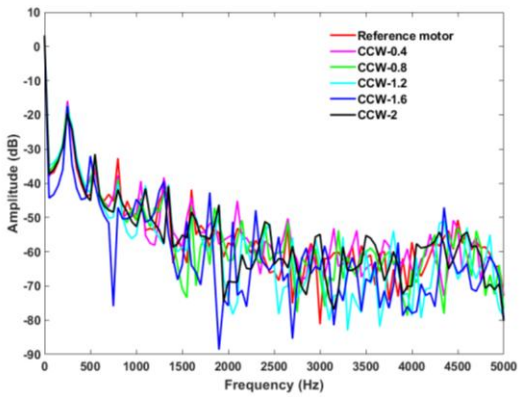

Figure 12. Torque spectrum of CCWs

As shown in Figure 12, when the result of the FFT analysis of the electromagnetic torque is analysed, significant changes are observed in the 250 Hz component of the torque spectrum compared to the reference conventional design, as in the CW models. This harmonic component has a value of 0.136 Nm in the reference motor; 17% increase in CCW-0.4 and 1% increase in CCW-0.8 compared to the reference motor; 14.7% decrease in CCW-1.2, 2.2% decrease in CCW-1.6 and 24.2% decrease in CCW-2. While this harmonic component increased by more than 60% in CW models, it decreased similar to torque ripple in CCW-1.2, CCW-1.6 and CCW-2 models. Another important component for torque ripple is known to be cogging torque. Figure 13 shows the cogging torque of the CCW models and the reference conventional BLDC motor.

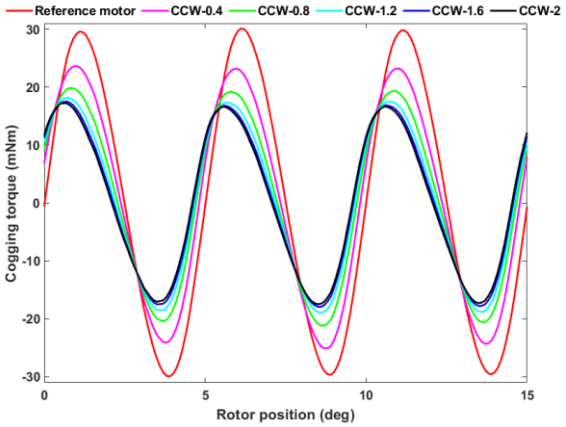

Figure 13. Cogging torque of CCWs

Among the cogging torques given in Figure 13, the reference motor has the highest value with 30 mNm. Compared to the reference conventional motor, the cogging torque decreased by 16.6% in CW-0.4 structure, 29.6% in CW-0.8 structure, 37% in CW-1.2 structure, 40.3% in CW-1.6 structure and 42% in CW-2 and decreased to 17.4 mNm. Considering all these, it is seen that with the asymmetric tooth structure in the stator, a decrease in cogging torque and a 4% increase in electromagnetic torque is achieved in CCW models, while torque ripple is improved, contrary to CW models.

5. Result and Discussion

In this study, an conventional outer rotor BLDCM for household electrical appliances is designed and analysed. In order to improve the performance of the designed motor, asymmetrical tooth structure and non-uniform air gap are used in the stator. Various asymmetric designs are investigated by FEM analyses in ANSYS program and the results are compared. Two different asymmetric structures, CW and CCW models, are evaluated and the results are given comparatively in Table 4.

Table 4. Comparison of analysis results

	Torque (Nm)	Torque ripple (%)	Cogging torque (mNm)	Cogging torque reduction (%)
Conventional motor	1.38	23.1	30	-
CW-2	1.57	33.1	17.9	40.3
CCW-2	1.43	19.4	17.4	42

According to Table 4, in CW models, it is observed that the asymmetric stator tooth structure increases the output torque, but also increases the torque ripple. The CW-2 model provided the highest output torque (13.7% increase), while the torque ripple reached the highest level with 33.1%. In addition, a 40.3% reduction in cogging torque is observed. CCW models both increased the output torque and reduced the torque ripple. The CCW-2 model provided the lowest torque ripple (19.4%) and a torque increase of 4%. In this model, the cogging torque decreased by 42%. CCW models provided better results in torque ripple compared to CW models.

This study lies in demonstrating that asymmetric stator tooth structures, particularly the CCW model, effectively enhance both output torque and reduce torque ripple and cogging torque, offering a cost-efficient solution for improving motor performance in household appliances. As a result, it is observed that the motors designed with asymmetric stator tooth structure provide significant improvements compared to the reference conventional outer rotor BLDC motors. CCW structures are more advantageous especially in torque ripple and cogging torque reduction. These designs offer a cost advantage due to the use of ferrite material while providing improvements

in noise and vibration levels. Considering that energy efficiency and sustainability issues remain important in the industry, it is predicted that such motor designs will become more widespread in the future.

Conflict of Interest

No conflict of interest was declared by the authors.

References

Hendershot, J. R., & Miller, T. J. E. (2010). *Design of Brushless Permanent- Magnet Machines*. Motor Design Books LLC.

Huang, X., Goodman, A., Gerada, C., Fang, Y., & Lu, Q. (2012). Design of a five-phase brushless DC motor for a safety critical aerospace application. *IEEE Transactions on Industrial Electronics*, *59*(9), 3532–3541. https://doi.org/10.1109/TIE.2011.2172170

Karan, V. K., Shekhar, S., Alam, A., & Thakur, A. (2024). Elimination of torque ripples by multiple slope ST-DTC vectors in PM-BLDC drive. *Electrical Engineering*, *106*(3), 3393–3402. https://doi.org/10.1007/s00202-023-02155-0

Khazaee, A., Zarchi, H. A., Markadeh, G. A., & Mosaddegh Hesar, H. (2021). MTPA Strategy for Direct Torque Control of Brushless DC Motor Drive. *IEEE Transactions on Industrial Electronics*, *68*(8), 6692–6700. https://doi.org/10.1109/TIE.2020.3009576

Kwack, J., Min, S., & Hong, J.-P. (2010). Optimal stator design of interior permanent magnet motor to reduce torque ripple using the level set method. *IEEE Transactions on Magnetics*, *46*(6), 2108–2111. https://doi.org/10.1109/TMAG.2010.2044871

Lee, S.-K., Kang, G.-H., Hur, J., & Kim, B.-W. (2012). Stator and rotor shape designs of interior permanent magnet type brushless DC motor for reducing torque fluctuation. *IEEE Transactions on Magnetics*, *48*(11), 4662–4665. https://doi.org/10.1109/TMAG.2012.2201455

Li, Z., Fan, X., Kong, Q., Liu, J., & Zhang, S. (2024). Torque Ripple Suppression of BLDCM With Optimal Duty Cycle and Switch State by FCS-MPC. *IEEE Open Journal of Power Electronics*, *5*(February), 381–391. https://doi.org/10.1109/OJPEL.2024.3368221

Lin, H., Wang, D., Liu, D., & Chen, J. (2014). Influence of magnet shape on torque behavior in surface-mounted permanent magnet motors. *2014 17th International Conference on Electrical Machines and Systems, ICEMS 2014*, 44–47. https://doi.org/10.1109/ICEMS.2014.7013448

Lipo, T. A. (2017). *Intorduction to AC Machine Design*. John Wiley & Sons Inc.

Liu, Y., Zhu, Z. Q., & Howe, D. (2005). Direct torque control of brushless DC drives with reduced torque ripple. *IEEE Transactions on Industry Applications*, *41*(2), 599–608. https://doi.org/10.1109/TIA.2005.844853

Mohanraj, D., Aruldavid, R., Verma, R., Sathiyasekar, K., Barnawi, A. B., Chokkalingam, B., & Mihet-Popa, L. (2022). A Review of BLDC Motor: State of Art, Advanced Control Techniques, and Applications. *IEEE Access*, *10*, 54833–54869. https://doi.org/10.1109/ACCESS.2022.3175011

Mohanraj, D., Gopalakrishnan, J., Chokkalingam, B., & Mihet-Popa, L. (2022). Critical Aspects of Electric Motor Drive Controllers and Mitigation of Torque Ripple - Review. *IEEE Access*, *10*(July), 73635–73674. https://doi.org/10.1109/ACCESS.2022.3187515

Park, J. H., & Lee, D. H. (2020). Simple Commutation Torque Ripple Reduction Using PWM with Compensation Voltage. *IEEE Transactions on Industry Applications*, *56*(3), 2654–2662. https://doi.org/10.1109/TIA.2020.2968412

Prabhu, N., Thirumalaivasan, R., & Ashok, B. (2023). Critical Review on Torque Ripple Sources and Mitigation Control Strategies of BLDC Motors in Electric Vehicle Applications. *IEEE Access*, *11*(October), 115699–115739. https://doi.org/10.1109/ACCESS.2023.3324419

Prakash, A., & Naveen, C. (2023). Combined strategy for tuning sensor-less brushless DC motor using SEPIC converter to reduce torque ripple. *ISA Transactions*, *133*, 328–344. https://doi.org/10.1016/j.isatra.2022.06.045

Rahman, M. M., Kim, K.-T., & Hur, J. (2014). Design and Optimization of Neodymium-Free SPOKE-Type Motor With Segmented Wing-Shaped PM. *IEEE Transactions on Magnetics*, *50*(2), 865–868. https://doi.org/10.1109/tmag.2013.2282151

Raja, M. S., & Geethalakshmi, B. (2018). Modified Rotor Material for Minimization of Torque Ripple for Interior Permanent Magnet BLDC motor. *Materials Today: Proceedings*, *5*(2), 3639–3647. https://doi.org/10.1016/j.matpr.2017.11.614

Rupam, Marwaha, S., & Marwaha, A. (2022). FEA Based Design of Outer Rotor BLDC Motor for Battery Electric Vehicle. *International Journal of Electrical and Electronics Research*, *10*(4), 1130–1134. https://doi.org/10.37391/ijeer.100459

Shi, T., Cao, Y., Jiang, G., Li, X., & Xia, C. (2017). A Torque Control Strategy for Torque Ripple Reduction of Brushless DC Motor with Nonideal Back Electromotive Force. *IEEE Transactions on Industrial Electronics*, *64*(6), 4423–4433. https://doi.org/10.1109/TIE.2017.2674587

Tezcan, M. M., & Yetgin, A. G. (2023). An Approach For Reducing Torque Ripples on Permanent Magnet Synchronous Motors : Slitted Stator Core. *Gazi Journal of Engineering Sciences*, *9*(2), 163–173. https://doi.org/10.30855/gmbd.0705061

Trivedi, M. S., & Keshri, R. K. (2020). Evaluation of Predictive Current Control Techniques for PM BLDC Motor in Stationary Plane. *IEEE Access*, *8*, 46217–46228. https://doi.org/10.1109/ACCESS.2020.2978695

Wang, L., Zhu, Z. Q., Bin, H., & Gong, L. (2021). A Commutation Error Compensation Strategy for High-Speed Brushless DC Drive Based on Adaline Filter. *IEEE Transactions on Industrial Electronics*, *68*(5), 3728–3738. https://doi.org/10.1109/TIE.2020.2984445

Xia, K., Ye, Y., Ni, J., Wang, Y., & Xu, P. (2020). Model predictive control method of torque ripple reduction for BLDC Motor. *IEEE Transactions on Magnetics*, *56*(1), 1–6. https://doi.org/10.1109/TMAG.2019.2950953

Yao, X., Zhao, J., Wang, J., Huang, S., & Jiang, Y. (2019). Commutation Torque Ripple Reduction for Brushless DC Motor Based on an Auxiliary Step-Up Circuit. *IEEE Access*, *7*, 138721–138731. https://doi.org/10.1109/ACCESS.2019.2943411